Journal of Sound and Vibration 401 (2017) 139–151

Contents lists available at ScienceDirect

Journal of Sound and Vibration

journal homepage: www.elsevier.com/locate/jsvi

Rolling bearing fault diagnosis based on time-delayed feedback monostable stochastic resonance and adaptive minimum entropy deconvolution

Jimeng Li [a,*], Ming Li [a], Jinfeng Zhang [b]

[a] College of Electrical Engineering, Yanshan University, Qinhuangdao 066004, PR China
[b] College of Liren, Yanshan University, Qinhuangdao 066004, PR China

ARTICLE INFO

Article history:
Received 19 December 2016
Received in revised form
17 April 2017
Accepted 25 April 2017
Handling Editor: K. Shin
Available online 29 April 2017

Keywords:
Rolling bearing fault diagnosis
Stochastic resonance
Monostable
Time-delayed feedback
Minimum entropy deconvolution

ABSTRACT

Rolling bearings are the key components in the modern machinery, and tough operation environments often make them prone to failure. However, due to the influence of the transmission path and background noise, the useful feature information relevant to the bearing fault contained in the vibration signals is weak, which makes it difficult to identify the fault symptom of rolling bearings in time. Therefore, the paper proposes a novel weak signal detection method based on time-delayed feedback monostable stochastic resonance (TFMSR) system and adaptive minimum entropy deconvolution (MED) to realize the fault diagnosis of rolling bearings. The MED method is employed to preprocess the vibration signals, which can deconvolve the effect of transmission path and clarify the defect-induced impulses. And a modified power spectrum kurtosis (MPSK) index is constructed to realize the adaptive selection of filter length in the MED algorithm. By introducing the time-delayed feedback item in to an over-damped monostable system, the TFMSR method can effectively utilize the historical information of input signal to enhance the periodicity of SR output, which is beneficial to the detection of periodic signal. Furthermore, the influence of time delay and feedback intensity on the SR phenomenon is analyzed, and by selecting appropriate time delay, feedback intensity and re-scaling ratio with genetic algorithm, the SR can be produced to realize the resonance detection of weak signal. The combination of the adaptive MED (AMED) method and TFMSR method is conducive to extracting the feature information from strong background noise and realizing the fault diagnosis of rolling bearings. Finally, some experiments and engineering application are performed to evaluate the effectiveness of the proposed AMED-TFMSR method in comparison with a traditional bistable SR method.

1. Introduction

Rotating machinery has played a significant role in the production of modern industry, such as wind turbines and machine tools. Rolling bearings, as core components, have been widely used in almost every rotating machinery. However, due to the influence of harsh environments and complex working conditions, they are prone to failure. The failure may

* Corresponding author.
E-mail address: xjtuljm@163.com (J. Li).

http://dx.doi.org/10.1016/j.jsv.2017.04.036
0022-460X/

deteriorate mechanical performance and even lead to fatal breakdowns. Therefore, they have received a lot of attention in the field of vibration analysis as they represent a common source of faults. In order to obtain valuable feature information from the vibration signals acquired by the transducers, various signal processing techniques, such as spectral kurtosis (SK) [1], empirical mode decomposition (EMD) [2], sparse representation [3], and wavelet transform (WT) [4], etc., have been extensively studied and applied in rolling bearing fault diagnosis. In comparison to these signal processing techniques for extracting useful features by filtering or masking noise, stochastic resonance (SR) regards noise as a kind of signal energy that realizes the extraction and enhancement of weak signal features by utilizing noise instead of eliminating noise. Consequently, SR provides an effective approach for weak features extraction in the mechanical fault diagnosis [5–7].

SR was originally presented by Benzi et al. to describe the periodicity associated with the Earth's ice ages in climatology in the 1980s [8]. And yet, in view of the good performance of SR using noise to enhance periodic signal features, SR-based fault diagnosis methods have been investigated in the last decade. Lei et al. proposed an adaptive SR method by using ant colony algorithm, and realized the fault diagnosis of planetary gearbox [9]. By introducing the wavelet packet transform into the multiscale noise tuning SR, Wang et al. presented an improved SR method particularly suited for the identification of multiple transient faults in rolling bearings [10]. In order to increase the calculation speed and noise utilization, Qin et al. [11] proposed an adaptive and fast SR method based on dyadic wavelet transform and least square parameters solving algorithm to extract the fault feature of a rotor system. Chen et al. studied a weak fault feature extraction method of planetary gear based on ensemble empirical mode decomposition (EEMD) and adaptive SR [12]. The effective intrinsic mode functions obtained by EEMD are selected and reconstructed, and then the reconstructed signal is processed by the adaptive SR method based on particle swarm optimization, thus realizing the weak feature extraction and fault diagnosis. Aiming at the shortcomings of multiscale noise tuning SR method based on discrete wavelet transform, Hu et al. [13] introduced the dual-tree complex wavelet transform into the multiscale noise tuning SR method, and realized the fault diagnosis of wind turbine drivetrain. Lai et al. [14] studied a SR method based on bistable Duffing oscillator, and solved the problem of large parameters signals detection to realize the incipient fault diagnosis of rotor system. These modified and optimized SR techniques have effectively promoted the development of SR theory and popularized the application of SR method in mechanical fault diagnosis.

However, it is worth noting that these engineering signal processing methods are almost all implemented in the framework of the bistable SR model. And in actual system there are a lot of monostable systems [15]. Therefore, some researches on the SR phenomenon in a monostable system have been conducted [16–18]. For example, Guo [19] studied the SR in a bias monostable system subject to frequency mixing force and multiplicative and additive noise based on adiabatic elimination theory, and obtained the analytic expression of the signal-to-noise ratio (SNR). Agudov et al. investigated the SR in an over-damped monostable system based on linear-response theory, and found that SNR was a nonmonotonic function of the noise intensity [20]. But the engineering application research is few about the SR method based on a monostable model in mechanical fault diagnosis. Furthermore, in consideration of the periodicity of weak signal to be detected, if the historical information can be used effectively in the SR system with a proper way, the periodic component in the SR output may be enhanced, i.e., weak signal detection performance is improved. Such an effect can be realized via a time-delayed feedback SR (TFSR) system [21]. The TFSR in a bistable system has been investigated in physical system and signal processing. However, the research on the TFSR in a monostable system is few, especially in the mechanical fault diagnosis. Therefore, this study combines the merits of the TFSR system and a monostable model, and presents a novel time-delayed feedback monostable SR (TFMSR) method to realize the engineering signal processing in rolling bearing fault diagnosis. The SR phenomenon of TFMSR system is demonstrated in theory, and analyzes the influence of time delay and feedback intensity on the SNR of system output. By selecting proper time delay, feedback intensity and re-scaling ratio with genetic algorithm, the SR output periodicity can be enhanced to realize the detection of weak periodic signal. On that basis, combined with the characteristics of rolling bearing vibration signals that the vibration signal collected by the transducer is the convolution between the defect-induced impulse response and the system transfer function, the minimum entropy deconvolution (MED) method [22,23] is adopted as the pretreatment way to effectively deconvolve the effect of the transmission path and clarify the impulses. And a modified power spectrum kurtosis (MPSK) index is constructed to evaluate the filtering effect of MED method, so that the filter length can be adaptively selected. By combining the adaptive MED (AMED) method and the TFMSR method, it is beneficial to extract the useful feature information from vibration signals in the fault diagnosis of rolling bearing. Finally, experiments and engineering application demonstrate that proposed AMED-TFMSR method in the paper is effective in the fault diagnosis of rolling bearings.

The rest of the paper is organized as followed: Section 2 mainly introduces the TFMSR method and AMED method in detail; and the algorithm flow of the proposed AMED-TFMSR method is described in Section 3. Then, Section 4 verifies the practicability of the proposed method by the experiments and engineering application, and provides further discussions. Finally, conclusions are drawn in Section 5.

2. Theoretical foundation

2.1. The model of TFMSR

SR describes a physical phenomenon that in a nonlinear system, the output SNR of the system increases to the maximum

and then decreases with the increase of noise intensity. It emphasizes the synergistic effect of the nonlinear system, small parameter signal and noise. Based on a classical bistable model, various SR methods and theories have been widely researched and applied in many fields. In this paper, consider an over-damped monostable system, and a time-delayed feedback item is introduced, thus the TFMSR system can be described by the following Langevin equation

$$\frac{\mathrm{d}x(t)}{\mathrm{d}t} = -\frac{\mathrm{d}U(x)}{\mathrm{d}x} + \beta x(t-\tau) + A\cos\Omega t + n(t) \tag{1}$$

in which, $x(t)$ represents the system output, parameters β and τ are the feedback intensity and the time delay respectively, $A\cos(\Omega t)$ is a periodic input signal with the amplitude A and the frequency $\Omega = 2\pi f_0$, and $n(t)$ is a Gaussian white noise with zero mean and D intensity. $U(x)$ is a reflection-symmetric quartic potential function as written as below

$$U(x) = \frac{b}{4}x^4(t) \tag{2}$$

where $b > 0$ is a system parameter. Substitute Eq. (2) into Eq. (1), we can get

$$\frac{\mathrm{d}x(t)}{\mathrm{d}t} = -bx^3(t) + \beta x(t-\tau) + A\cos\Omega t + n(t) \tag{3}$$

Eq. (3) indicates that the system response $x(t)$ of SR is essentially the solution of differential equation that is obtained by integral calculation. And the integral can smooth the high-frequency dithering of input signal, thereby SR can be regarded as a special low-pass filter. Furthermore, it can be found from Eq. (3) that apart from the system parameter b, the introduced time delay τ and feedback intensity β also affect the system output along with the signal filtering performance. Therefore, the next step is to analyze the relationship among the system response of SR and the control parameters via the adiabatic limitation approach. It is noted that the following formula derivation of TFMSR is under the condition of small time delay [24,25].

Let $P(x, t)$ represent the probability density of the stochastic process defined by Eq. (3) at time t, and then the delay Fokker-Planck equation for the probability density can be written as [26]

$$\frac{\partial P(x,t)}{\partial t} = -\frac{\partial\left[h_{eff}P(x,t)\right]}{\partial x} + D\frac{\partial^2 P(x,t)}{\partial x^2} \tag{4}$$

where h_{eff} is the conditional average drift that can be expressed as

$$h_{eff} = \sqrt{\frac{1}{4\pi D\tau}}\int_{-\infty}^{+\infty}\mathrm{d}x_\tau h(x, x_\tau)\times\exp\left(-\frac{\left[x_\tau - x - h^{(0)}(x)\tau\right]^2}{4D\tau}\right) \tag{5}$$

where $x_\tau = x(t-\tau)$, $h(x, x_\tau) = -bx^3 + \beta x_\tau + A\cos\Omega t$, $h^{(0)}(x) = -bx^3 + \beta x + A\cos\Omega t$. And substitute x_τ, $h(x, x_\tau)$ and $h^0(x)$ into Eq. (5), h_{eff} can be obtained [24,25]

$$h_{eff} = -(1+\beta\tau)\left(bx^3 - \beta x\right) + (1+\beta\tau)A\cos\Omega t \tag{6}$$

In the absence of input signal, by integrating Eq. (6), the equivalent potential function $U_e(x)$ can be given by

$$U_e(x) = (1+\beta\tau)\left(\frac{b}{4}x^4 - \beta\frac{x^2}{2}\right) \tag{7}$$

Comparing Eq. (7) with Eq. (2), it can be observed that the original monostable potential is transformed into a bistable potential by introducing the time-delay feedback item. Fig. 1 illustrates the potential function $U_e(x)$ with different parameters β and τ on the premise of parameter b=0.2. As seen from Fig. 1(a), when parameter $\beta > 0$, the potential function $U_e(x)$ has two potential wells, and the depth of potential well decreases with a decreasing value of parameter β. However, the potential function $U_e(x)$ will gradually lose its bistability and become a monostable model when parameter β is less than or equal to 0. Fig. 1(b) shows that the depth of potential well increases with a increasing value of parameter τ on the premise of parameter $\beta > 0$. Therefore, by adjusting the parameters β and τ, the structure of potential function $U_e(x)$ can be changed, thus affecting the performance of periodic signal extraction from background noise.

Subsequently, according to the calculation formula of the probability transition rate for Brownian particle motion in a symmetric two-dimensional bistable system [27], under the condition of weak noise, the probability transition rate for Brownian particle transition between the two potential wells can be calculated by using Eqs. (8) and (9).

$$R_{\pm}(t) = r_k\exp\left(\mp\frac{\sqrt{\beta/b}(1+\beta\tau)A}{4D}\cos\Omega t\right) \tag{8}$$

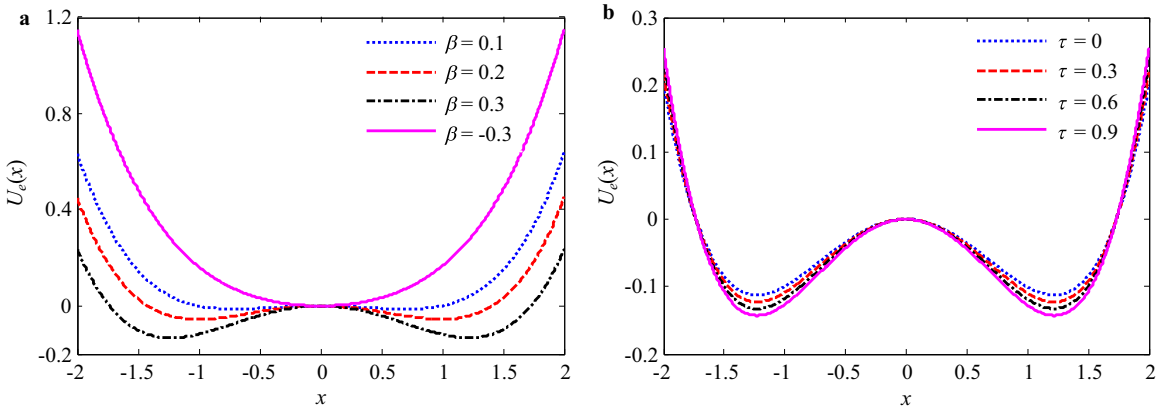

Fig. 1. The equivalent potential function $U_e(x)$: (a) the change trend of $U_e(x)$ versus parameter β with constant parameter τ=0.6; (b) the change trend of $U_e(x)$ versus parameter τ with constant parameter β=0.3.

$$r_k = \frac{\beta(1+\beta\tau)}{\sqrt{2}\pi}\exp\left(-\frac{\beta^2(1+\beta\tau)}{4bD}\right) \tag{9}$$

in which R_+ and R_- represent the probability transition rate of the Brownian particle from the right (left) potential well to the left (right) potential well, respectively.

Based on the method of rate equation in the adiabatic limit and the theory of two-state model, by substituting Eqs. (8) and (9) into the formula of the two-state model with potential Eq. (7) [27], the power spectrum density of output variable can be obtained as

$$S(\omega) = \int_{-\infty}^{\infty}\langle x(t)x(t+\tau)\rangle e^{-j\omega\tau}d\tau = S_1(\omega) + S_2(\omega) \tag{10}$$

where $S_1(\omega)$ and $S_2(\omega)$ represent that the output power spectra of the signal and noise, respectively, and can be expressed as

$$S_1(\omega) = \frac{\beta\pi}{2b}\left(\frac{(1+\beta\tau)A\sqrt{\beta/b}}{D}\right)^2\frac{4r_k^2}{4r_k^2+\Omega^2}[\delta(\omega-\Omega)+\delta(\omega+\Omega)] \tag{11}$$

$$S_2(\omega) = \left[1 - \frac{A^2\beta(1+\beta\tau)^2 4r_k^2}{2bD^2\left(4r_k^2+\Omega^2\right)}\right]\frac{4\beta r_k}{b\left(4r_k^2+\omega^2\right)} \tag{12}$$

Finally, the SNR of the TFMSR system is defined as

$$SNR = \frac{P_s}{S_2(\omega=\Omega)}, \quad P_s = \int_0^{\infty} S_1(\omega)d\omega \tag{13}$$

By substituting Eq. (11) and Eq. (12) into Eq. (13), the SNR can be obtained as

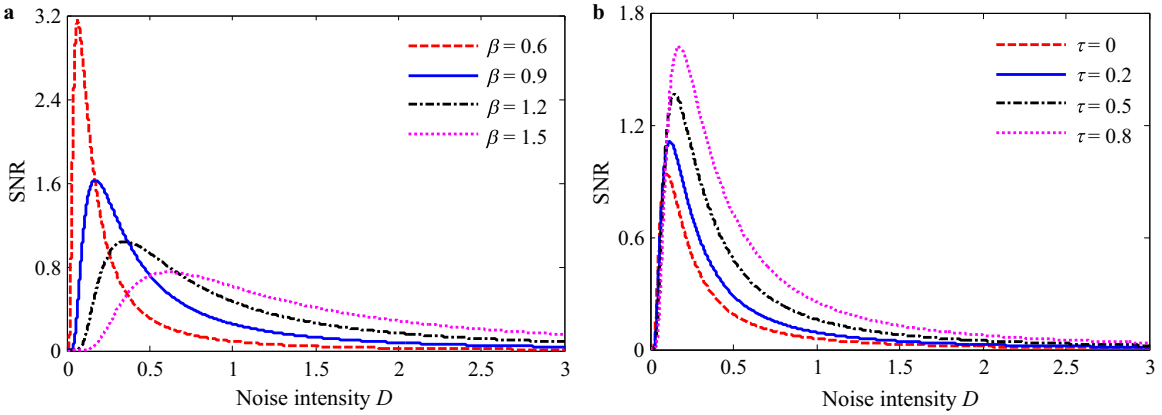

Fig. 2. The change trends of SNR versus noise intensity: (a) A=0.5, b=1, τ=0.8; (2) A=0.5, b=1, β=0.9.

$$SNR = \frac{\sqrt{2}A^2\beta^2(1+\beta\tau)^3}{4bD^2}\exp\left(-\frac{\beta^2(1+\beta\tau)}{4bD}\right) \tag{14}$$

Fig. 2 illustrates the change curves of SNR versus noise intensity with different parameters β and τ, all of which are first increased and then decreased with the variation in noise intensity and show the celebrated nonmonotonic characteristics. Furthermore, the maximum of SNR is gradually decreased with the increase of parameter β, as shown in Fig. 2(a). Conversely, Fig. 2(b) indicates that the maximum of SNR increases when parameter τ is increased gradually. The analyzed results show that the SNR of system output is affected by the time delay τ and feedback intensity β. Consequently, we can select appropriate control parameters τ and β, namely that adjust the structure of the potential $U_e(x)$, to optimize the output SNR of TFMSR system, thus realizing the feature extraction of weak signal from background noise. In addition, it is noted that the time delay τ represents a continuous time variable in the above theoretical analysis, but in the numerical solution of differential equation and engineering signal processing, τ is a discrete value which represents data points.

2.2. The method of AMED

In a rolling bearing, when a rolling element strikes a localized defect, an impulse occurs and this excites the resonances of the structure. If the effect of the transmission path on the defect-induced impulse responses can be eliminated/deconvolved in the vibration signal collected by the vibration transducer, it is beneficial to extract the feature information and perform the fault diagnosis. The MED method was first introduced by Wiggins [28] to aid the extraction of detailed reflectivity information from amplitude anomalies in seismic data. It can recover the output signal with the maximum value of kurtosis index by searching for an optimum set of filter coefficients. As a non-dimensional index, kurtosis index is an indicator that reflects the "peakedness" of a signal, and therefore the property of impulses. Therefore, the MED method has been used effectively to enhance the impulses in a mixture signal [22,29]. Fig. 3 illustrates the deconvolution process of the MED method.

In Fig. 3, the signal $g(k)$ represents the original impulses generated by faulty rolling bearing, $h(k)$ represents the effect of transmission path on the signal $g(k)$, and $n(k)$ represents the noise interference. Thus the vibration signal $x(k)$ collected by the vibration transducer can be expressed as:

$$x(k) = \big(g(k) + n(k)\big)*h(k) \tag{15}$$

where the symbol $*$ denotes the convolution operation. In order to recover/deconvolved the impulses signal $g(k)$ from the mixed signal $x(k)$, the objective of the MED method is to find the coefficients of the inverse filter $f(i)$ which makes the objective function $O_4\big(f(i)\big)$ maximum. The detailed solution procedure of MED algorithm has been presented in references [22,29].

$$y(k) = \sum_{i=1}^{L} f(i)x(k-i) \tag{16}$$

$$O_4\big(f(i)\big) = \sum_{k=1}^{N} y^4(k) \Big/ \left[\sum_{k=1}^{N} y^2(k)\right]^2 \tag{17}$$

Eq. (16) indicates that the length L of inverse filter $f(i)$ has important influence on the extraction effect of $y(k)$. However, the length L of filter, as the important parameter of MED method, needs to be specified in advance. And there is no unified standard to guide how to select the appropriate length L of filter. Consequently, by comparing the statistical indexes of time- and frequency-domain, the power spectrum kurtosis (PSK) index and margin index (MI) are selected to construct a new measurement index, which is applied to evaluate the extraction effect of impulses by using the MED filter with different lengths, so as to select the optimal length L of filter adaptively.

Fig. 4(a) displays the change trends of PSK and MI versus noise intensity for periodic impact signal quantitative characterization. It can be found that the two indexes are first decreased and then leveled off gradually with the increasing of

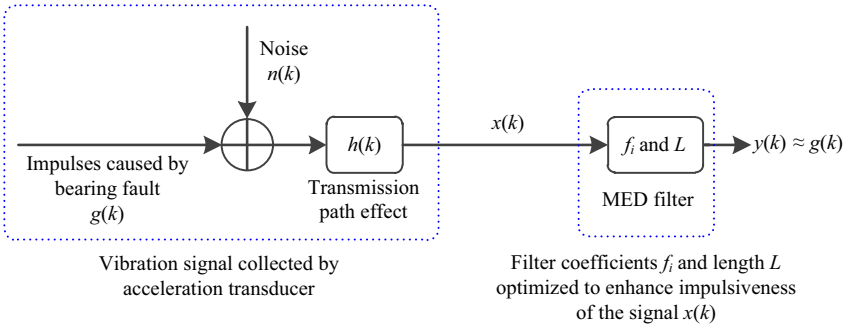

Fig. 3. Process schematic of MED algorithm.

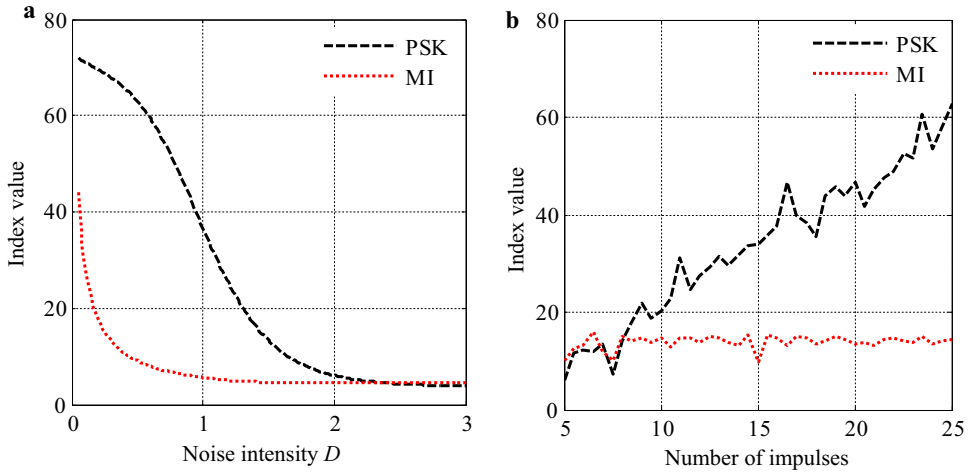

Fig. 4. The change trends of PSK and MI versus noise intensity and impulse number.

noise intensity. However, the variation tendencies of both are different, MI changes rapidly and the corresponding index value increases quickly with the decreasing of noise intensity. This illustrates that with the decreasing of noise intensity, MI has better characterization capability for periodic impact components in vibrations signals. Fig. 4(b) shows the influence of the number of impulses on the two indexes. As the number of impulses increases, PSK is increased gradually, while the change of MI is relatively steady. It indicates that PSK, as a frequency domain statistical index, can better reflect the characteristics of periodic impact components in vibration signal. These analysis results demonstrate that for the quantitative detection of the periodic impact components in vibration signal, MI is more sensitive to the change of noise, and PSK index has strong quantitative characterization capability for periodic impact components. Therefore, by combining PSK index with MI, a MPSK index is presented in paper, which can be defined as follows

$$\mathrm{MPSK} = \frac{\frac{N}{2}\sum_{k=1}^{N/2}(X(k)-\bar{X})^4}{\left(\sum_{k=1}^{N/2}(X(k)-\bar{X})\right)^2} \bullet \frac{x_p}{\left(\frac{1}{N}\sum_{i=1}^{N}\sqrt{|x_i|}\right)^2} \tag{18}$$

where, $X(k)$ is the amplitude sequence of power spectrum of $x(n)$, $\bar{X}$ denotes the mean value of $X(k)$, $x_p = E\left[\max\{x(n)\}\right]$, N is the length of signal, $x(n)$ is the discrete signal sequence. The MPSK index not only can quantitatively evaluate the extraction effect of periodic impact components from vibration signal, but also inherits the sensitivity of MI to noise.

Fig. 5 indicates the change trends of MPSK and PSK versus noise intensity. It can be observed that the variation tendencies of both are different, MPSK changes rapidly and the corresponding index value increases quickly with the decreasing of noise intensity. This demonstrates that with the decreasing of noise intensity, the MPSK has better characterization capability for periodic impact components in vibrations signals, whose sensitivity is higher than that of PSK. According to the principle of MED method, as shown in Fig. 3, if an appropriate filter length L is selected, the noise contained in

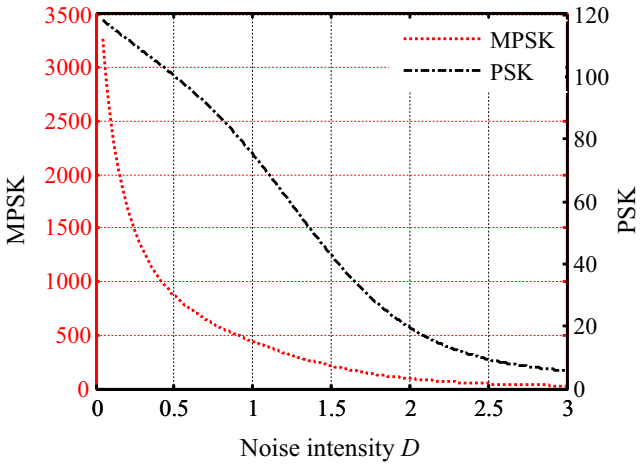

Fig. 5. The change trends of MPSK and PSK versus noise intensity.

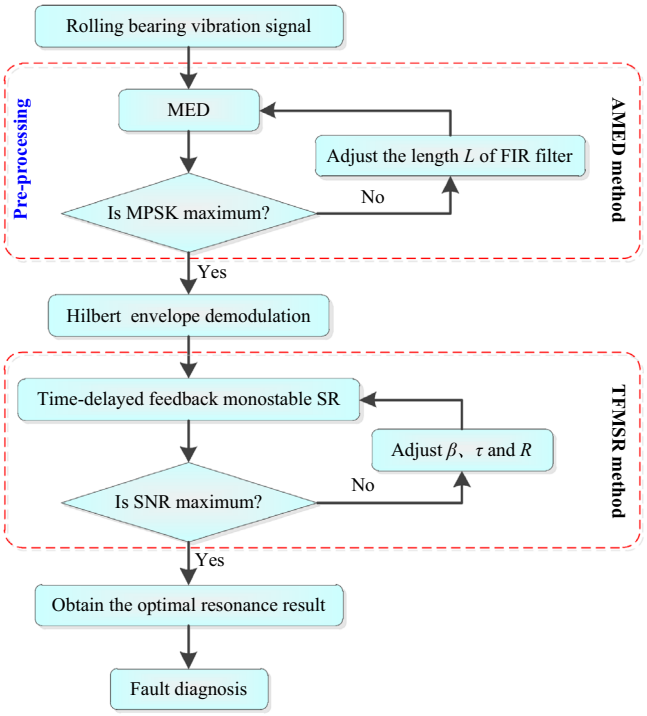

Fig. 6. The algorithm flow chart of AMED-TFMSR method.

vibration signal can be filtered to the greatest extent, and the optimal filtering result of periodic impact signal can be obtained. Therefore, based on the good characterization capability of MPSK index for periodic impact components in vibration signal, an adaptive MED (AMED) method is proposed by combining the MED method and the MPSK index in the paper. And the MPSK index is applied to evaluate the extraction effect of impulses by using the MED filter with different lengths, and the optimal length L of filter can be determined based on the MPSK maximum of filtering result $y(k)$ through iterative search, so as to effectively deconvolve the impulses from a mixture of response signals.

3. The algorithm flow of AMED-TFMSR method

Given the above, based on the advantages of SR detecting periodic signal (i.e., sine/cosine signal), the algorithm procedure of the proposed AMED-TFMSR method is illustrated in Fig. 6, as described in the following steps:

(1) Pre-processing with the AMED method. First, the original vibration signal x is processed by the AMED method, and the length L of MED filter is optimized and selected by maximizing the MPSK of filtering result, to obtain the optimal output y. And then, calculated the MPSK of the original signal x, and if the MPSK of filtering result y is greater than that of original signal x, the filtering result y is used as the input of Hilbert envelop demodulation, otherwise the original signal x is processed directly by the Hilbert transform.
(2) Hilbert envelop demodulation. The Hilbert envelop analysis is applied to demodulate the vibration signal collected from the rolling bearings, and the obtained envelope signal is inputted into the time-delayed feedback monostable SR system.
(3) Adaptive TFMSR method. First, set the searching ranges of control parameters β, τ and the re-scaling ratio R with system parameter $b=1$, and the initial parameters of genetic algorithm. And then, the genetic algorithm is applied to adaptively select and optimize control parameters, whose fitness function is constructed using SNR of resonance output, as shown Eq. (19). Finally, the best resonance result is obtained by maximizing the SNR of resonance output.

$$\mathrm{SNR} = 20\log_{10}\frac{A_d}{A_n} \tag{19}$$

where A_d is the amplitude value corresponding to the driving signal frequency, and A_n is the maximum values except A_d in the amplitude spectrum.
(4) Fault diagnosis. Combined with the mechanical equipment parameters information, the health conditions of rolling bearings can be identified and diagnosed with SR detection results.

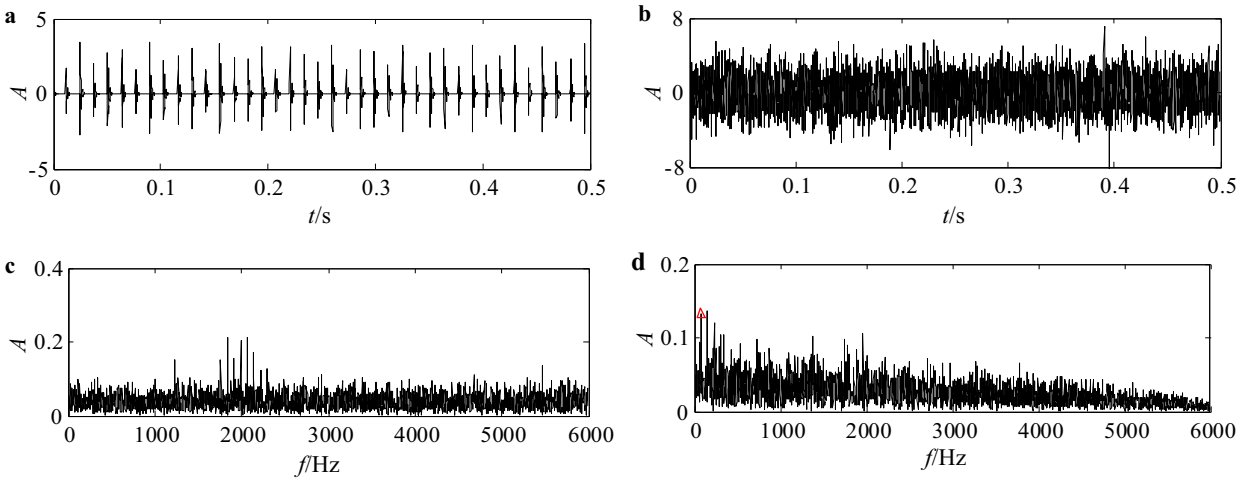

Fig. 7. The simulation signal: (a) the original waveform of impact signal; (b) the time waveform of mixed signal $x(t)$; (c) the spectrum of signal $x(t)$; (d) Hilbert envelop spectrum of signal $x(t)$.

4. Experimental verification and engineering application

In this section, some experimental data and generator bearing vibration data of wind turbine have been analyzed to demonstrate the effectiveness of the proposed method in mechanical fault diagnosis.

4.1. Numerical simulation and experimental verification

4.1.1. Numerical simulation

In this subsection, the proposed AMED-TFMSR method is adopted to detect weak periodic impact features from strong noise. The simulation signal is defined as

$$\begin{cases} x(t) = e^{-\alpha t_1}\sin(2\pi f_1 t_1)\times(\sin(2\pi f_2 t)+3)+n(t) \\ t_1 = \mathrm{mod}(t, 0.98/f_m) \end{cases} \tag{20}$$

where, $\alpha=1000$ denotes the decay factor, $f_1=2000$ Hz is the resonant frequency, $f_2=30$ Hz is the rotating frequency, and $f_m=75$ Hz is the fault frequency (the reciprocal of impact period). $n(t)$ is Gaussian white noise with zero-mean and 1.7 standard deviation. The sampling frequency is 12,000 Hz, and the length of data is 6000 points. Fig. 7(a) displays the original periodic impact signal, and the time waveform of mixed signal $x(t)$ and its corresponding spectra are shown in Fig. 7 (b)–(d). Obviously, the periodic impact signal is completely submerged by strong noise, the useful feature information such as the fault frequency cannot be found in Fig. 7(c). And in the Hilbert envelop spectrum as shown in Fig. 7(d), an unobvious spectrum peak at the fault frequency denoted by a red triangle can be found, but it is not enough to diagnose the fault.

The proposed AMED-TFMSR method is applied to analyze the simulation signal according to the algorithm flow shown in Fig. 6. The length of MED filter is optimized and selected based on the maximum of MPSK of filtering result. And in the adaptive TFMSR method, the genetic algorithms parameters settings: the number of initial population is 50, and the searching ranges of feedback intensity β, time delay τ and re-scaling ratio R are $[-10, 10]$, [1,500] and [10,2000] respectively, the maximum number of generations is 30 and the precision of the variables is 1e-8, etc. The corresponding detection results obtained by the proposed method are displayed in Fig. 8. Fig. 8(a) and (b) show the processing results of AMED method. Although the time waveform shown in Fig. 8(a) still cannot provide the valuable information, the spectrum peak at 76.11 Hz which is close to the fault frequency in Fig. 8(b) is more evident than that in Fig. 7(d). This illustrates that some noise contained in the original signal is filtered, and the impact features are enhanced by the AMED method. Fig. 8(c) displays the time waveform of resonance output of the proposed method, and the spectrum peak at 76.11 Hz is very prominent in Fig. 8(d), and the noise and some interference components are reduced significantly compared to Fig. 8(b). Consequently, the proposed method can realize the effective extraction of weak feature information from strong background noise.

4.1.2. Vibration data of rolling bearing from bearing test rig

In order to demonstrate the effectiveness of the proposed AMED-TFMSR method in the paper, the experimental data collected from the locomotive bearing test rig was adopted to be analyzed. And the test bearing with a local rub on outer race was installed in a hydraulic motor driven mechanical system. The sampling frequency was 12,800 Hz, and the shaft speed was 380 r/min. The rolling bearing parameters are listed in Table 1, and the fault characteristic frequency of bearing outer race is 45.7 Hz. The defective bearing is illustrated in Fig. 9.

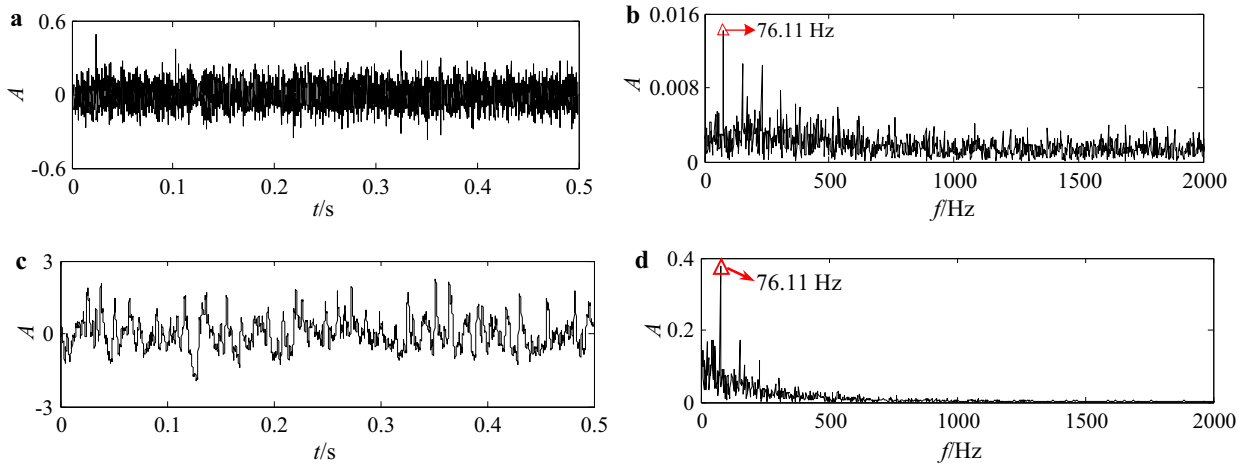

Fig. 8. The detection results of the proposed method: (a) the output waveform of AMED method; (b) Hilbert envelop spectrum of AMED output; (c) the resonance output waveform; (d) the spectrum of resonance output.

The time waveform of defective bearing vibration signal and its corresponding spectra are displayed in Fig. 10. Obviously, the useful feature information is completely corrupted by strong noise in Fig. 10(a). Furthermore, the frequency components are abundant, making it hard to discover the feature information relevant to the outer race fault of rolling bearing in Fig. 10(b). In the Hilbert envelop spectrum, as shown in Fig. 10(c), a spectrum peak at 46 Hz which is approximately consistent with the fault characteristic frequency of bearing outer race can be found, but it is less obvious because of the influence of background noise.

The vibration signal of defective bearing is processed by the proposed method with the same algorithm parameters as before, and Fig. 11(a) and (b) illustrate the time waveform of resonance output and the corresponding spectrum. It is observed that the spectrum peak at 46 Hz corresponding to the outer race fault characteristic frequency of rolling bearing is very prominent in Fig. 11(b), and lots of background noise is significantly reduced, the output SNR is 3.28 dB. In addition, Fig. 11(c) and (d) display the detection results of the adaptive TFMSR method for the vibration signal of rolling bearing. That is, in the algorithm flow of the proposed method shown in Fig. 6, the pre-processing with the AMED method is removed. It is clearly that it still contains lots of noise, as shown in Fig. 11(c). Although the feature frequency relevant to the bearing outer race fault can be found in Fig. 11(d), the output SNR is lower than that of Fig. 11(b), i.e. the detection performance of TFMSR method for the weak signal is inferior to that of the proposed AMED-TFMSR method. Meanwhile, the processing results of the traditional bistable SR method for the vibration signal are illustrated in Fig. 11(e) and (f). The comparison results demonstrate that the proposed AMED-TFMSR method can effectively eliminate the interference of useless components, and realize the enhanced extraction of feature information in the fault detection of rolling bearing.

Table 1
Rolling bearing parameters.

Bearing type	Pitch diameter D/mm	Roller diameter d/mm	Number of roller	Contact angle β/(°)
552732QT	225	34	17	0

Fig. 9. The rolling bearing with defective outer race.

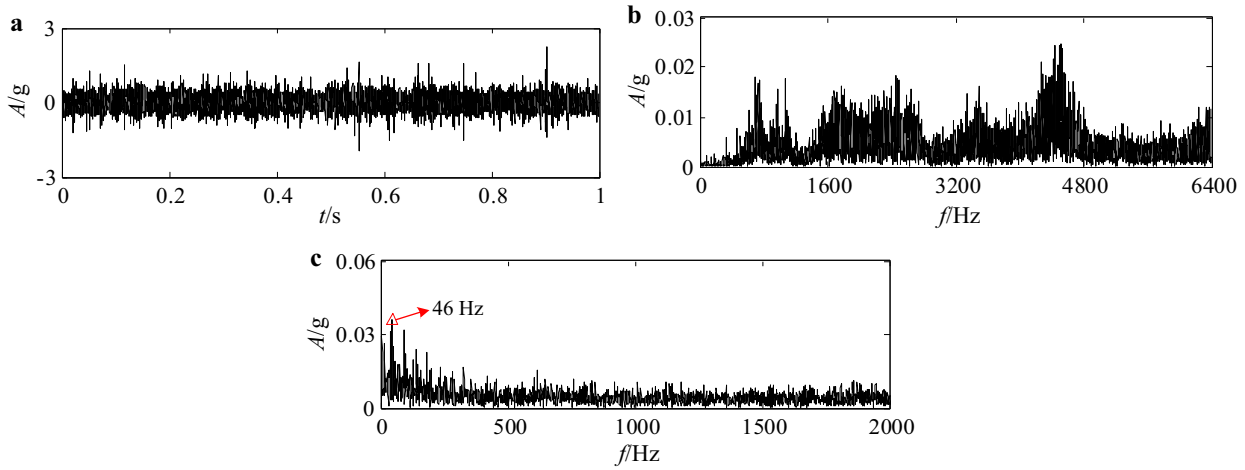

Fig. 10. The vibration signal of rolling bearing: (a) the time waveform; (b) the spectrum; (c) Hilbert envelop spectrum.

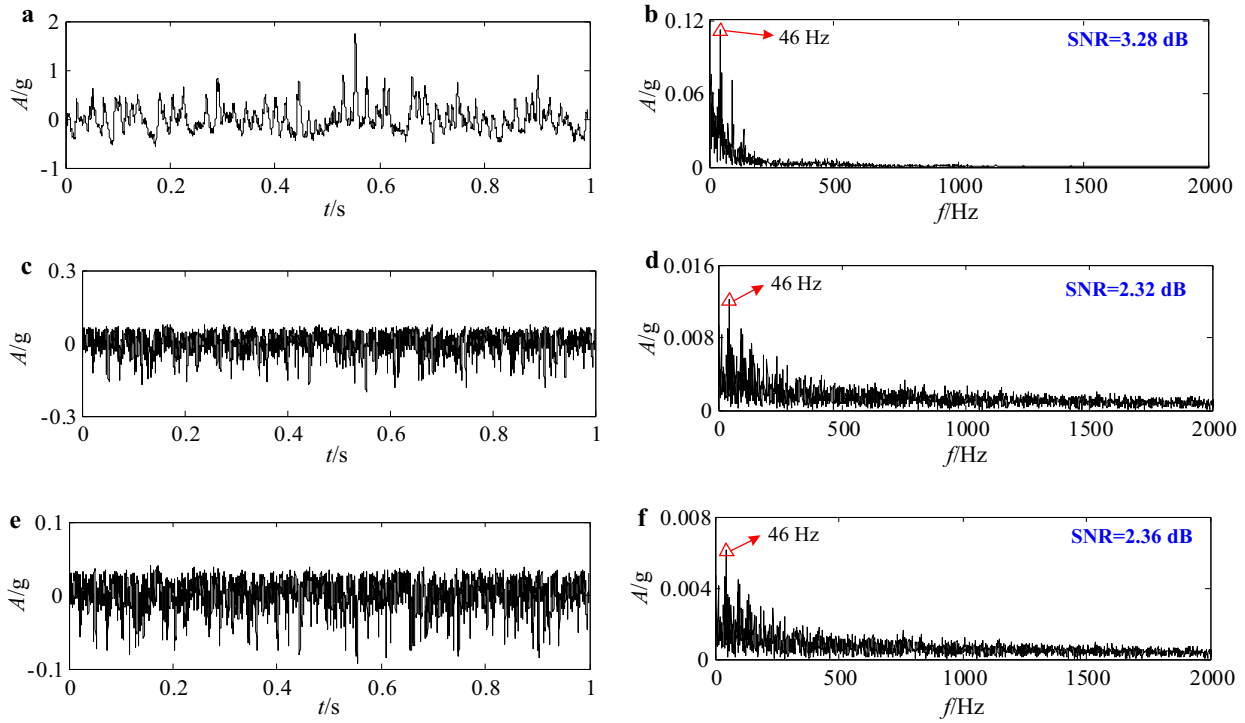

Fig. 11. The detection results: (a) the resonance output of the proposed method; (b) the output spectrum of the proposed method; (c) the resonance output of the TFMSR method; (d) the output spectrum of the TFMSR method; (e) the resonance output of the traditional bistable SR method; (f) the output spectrum of the traditional bistable SR method.

4.2. Engineering application for bearing fault diagnosis of wind turbine

Wind energy, as a clean and renewable energy, has brought the widespread attention all over the world, which is conducive to ameliorating and alleviating the serious environment problems and energy crisis in recent years. However, the transmission system failure of wind turbine occurred frequently, and the high operation and maintenance costs has become an important factor of affecting the economic benefit of wind power. Consequently, the condition monitoring and fault diagnosis for wind turbine is increasingly becoming the focus of manufacturers and wind-farm operators. Generator, serves as the important component of wind turbine, is prone to failure because of the influence of complex conditions. And noisy work environments and strong electromagnetic interference make the useful information relevant to mechanical fault in vibration signal acquired from the generator be submerged, thus increasing the difficulty of detecting fault. Therefore, the proposed method in the paper is used for the fault diagnosis of generator bearing in wind turbine, to achieve the extraction

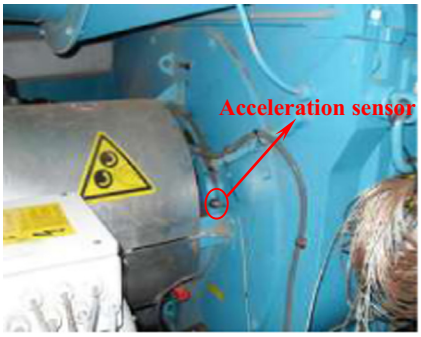

Fig. 12. The installation location of the acceleration sensor on the front bearing of generator.

Table 2
Generator bearing parameters of wind turbine.

Bearing type	Inner diameter D_i/mm	Outer diameter D_o/mm	Roller diameter d /mm	Number of roller	Contact angle β/(°)
6324	120	280	41.275	8	0

and enhancement of feature information.

Through the regular detection for wind turbines in a wind farm, it was found that the abnormal vibration was occurred in the front bearing of generator of No. 8 wind turbine. Fig. 12 shows the installation location of the acceleration sensor on the front bearing of generator. And the bearing parameters of generator are displayed in Table 2. The sampling frequency was 12,800 Hz, and the length of data was 16,384. The average rotational speed of the generator was 1406 r/min.

The time waveform of generator bearing vibration signal is shown in Fig. 13(a), and several irregular impulse components can be found, but fails to provide the useful information for fault identification. In the spectrum, as shown in Fig. 13(b), except for the rotating frequency 23.44 Hz, the feature frequency information relevant to bearing fault also cannot be discovered. In Fig. 13(c), besides the rotating frequency, it can be found a spectrum peak at 113.3 Hz, which consists with the fault characteristic frequency of bearing inner race. However, due to the influence of interference components, features of the useful information are not be evident enough to detect faults.

The proposed method is applied to analyze the bearing vibration signal, and the algorithm parameters are the same as the previous section. The detection results are displayed in Fig. 14. It is observed that the spectrum peak at 113.3 Hz is prominent in the spectrum as shown in Fig. 14(b), and the output SNR is 2.81 dB. The decibel value corresponding to the fault characteristic frequency of bearing inner race calculated by using Shock Pulse Method is 21.64 dB, which indicates there is an early damage on the bearing inner race.

Similarly, the vibration signal of generator bearing is also processed by the TFMSR method and the traditional bistable SR

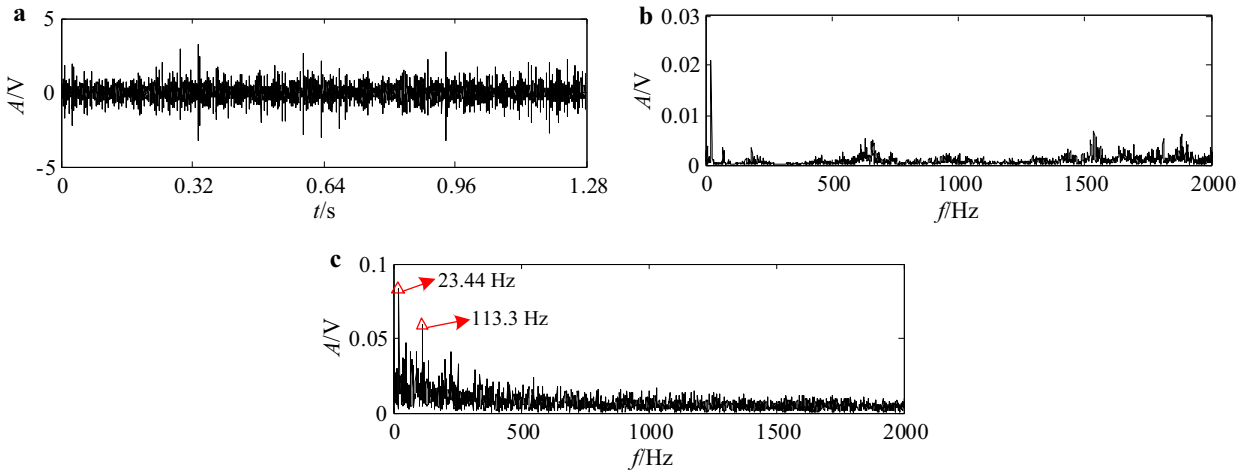

Fig. 13. The vibration signal of generator bearing of wind turbine: (a) the time waveform; (b) the spectrum; (c) Hilbert envelop spectrum.

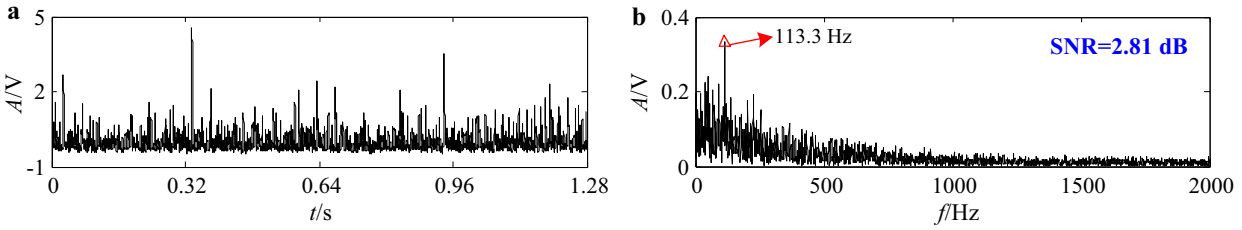

Fig. 14. The detection result of the proposed method: (a) the resonance output waveform; (b) the spectrum of resonance output.

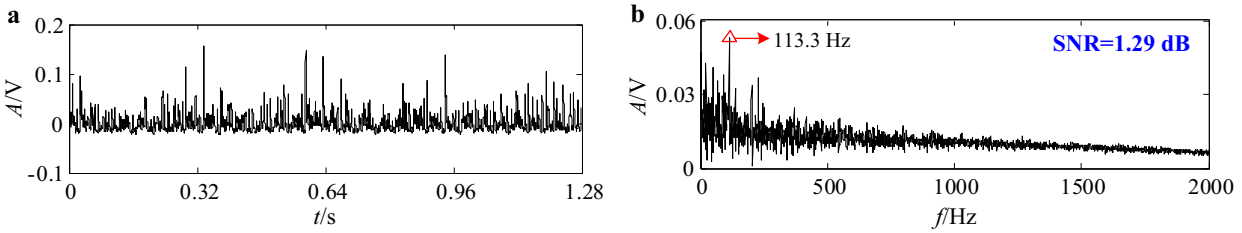

Fig. 15. The detection result of the TFMSR method: (a) the resonance output waveform; (b) the spectrum of resonance output.

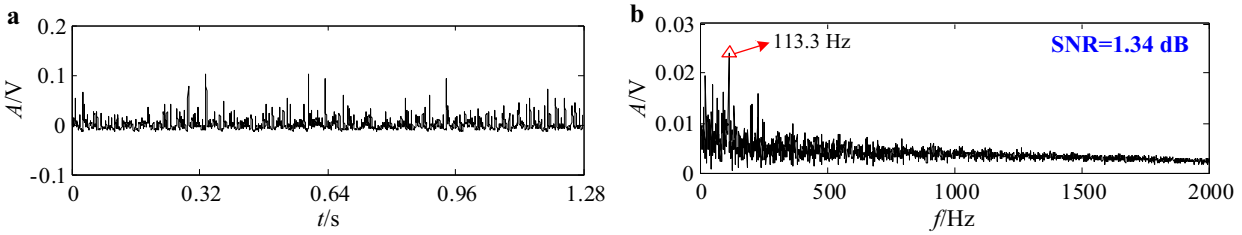

Fig. 16. The detection result of the traditional bistable SR method: (a) the resonance output waveform; (b) the spectrum of resonance output.

method, respectively. And the comparison results are displayed in Fig. 15 and Fig. 16. Obviously, although the two methods can also extract the feature frequency relevant to the bearing inner race fault, the output SNRs are lower than that of the proposed method. Therefore, the proposed method has superiority in enhancing performance in the fault detection of rolling bearing, and is suited for applications involving weak fault diagnosis.

4.3. Discussion

(1) This paper investigated the SR in a reflection-symmetric quartic potential monostable over-damped system based on adiabatic limitation approach. From the derivation, it is found that the monostable potential function $U(x)$ can be equivalent to a bistable potential function $U_e(x)$ by introducing a time-delayed feedback item into the monostable system. And changing the parameters of time delay and feedback intensity is to adjust the structure parameters of potential $U_e(x)$. Based on parameter-induced SR theory, the occurrence of SR can be manipulated by changing the structure parameters of bistable potential. Therefore, from another aspect, we can also conclude that the TMFSR system can produce SR phenomenon by adjusting the time delay and feedback intensity.

(2) It can be observed from the previous analysis that the influence of feedback intensity on potential structure is larger than that of time delay. And the potential $U_e(x)$ can be switched between the monostability and bistability by adjusting the feedback intensity. When the feedback intensity $\beta > 0$, the potential $U_e(x)$ shows the bistability, otherwise it becomes a monostable model.

(3) The MED method is employed to deconvolve the effect of the transmission path on the vibration signal, but how to select the proper filter length is still an open problem. Although the paper realizes the adaptive selection of filter length by constructing a MPSK index, the filtering effect is not very satisfactory and the problem-solving strategy needs further improvement. Consider also using other signal processing methods (e.g., SK, maximum correlated kurtosis deconvolution [30]) to be as the pretreatment way, thereby further enhancing the weak signal detection performance of TFMSR method.

5. Conclusion

This paper presents an AMED-TFMSR method to enhance the weak signal detection in rolling bearing fault diagnosis. By constructing a MPSK index to evaluate the filtering effect of MED method for vibration signal, the length of filter can be optimized and selected adaptively, which is beneficial to deconvolve the effect of transmission path and clarify the defect-induced impulses. By introducing a time-delayed feedback item into an over-damped monostable system, the influence of time delay and feedback intensity on the SR phenomenon is analyzed. And the results show that the SR can be manipulated by adjusting the time delay and feedback intensity, and the weak signal detection performance can be improved by using the historical information. Finally, experiments and engineering application demonstrate the effectiveness and superiority of the proposed method. Furthermore, it can be concluded that through the combination of the AMED method and TFMSR method, the proposed method can obtain better detection performance for rolling bearing fault diagnosis.

Acknowledgement

This work was supported by the National Natural Science Foundation of China (Grant no. 51505415), China Postdoctoral Science Foundation Funded Project (Grant no. 2015M571279), Hebei Province Natural Science Foundation of China (Grant nos. E2017203142 and F2016203421), and Science and Technology Support Project of Qinhuangdao City (Grant no. 201602A025). The authors would like to thank the anonymous reviewers for their valuable comments and suggestions.

References

[1] Y.X. Wang, J.W. Xiang, R. Markert, M. Liang, Spectral kurtosis for fault detection, diagnosis and prognostics of rotating machines: a review with applications, Mech. Syst. Signal Process. 66–67 (2016) 679–698.
[2] Y. Lv, R. Yuan, G.B. Song, Multivariate empirical mode decomposition and its application to fault diagnosis of rolling bearing, Mech. Syst. Signal Process. 81 (2016) 219–234.
[3] G.L. He, K. Ding, H.B. Lin, Fault feature extraction of rolling element bearings using sparse representation, J. Sound Vib. 366 (2016) 514–527.
[4] C.L. Zhang, B. Li, B.Q. Chen, H.R. Cao, Y.Y. Zi, Z.J. He, Weak fault signature extraction of rotating machinery using flexible analytic wavelet transform, Mech. Syst. Signal Process. 64–65 (2015) 162–187.
[5] X.F. Zhang, N.Q. Hu, Z. Cheng, L. Hu, Enhanced detection of rolling element bearing fault based on stochastic resonance, Chin. J. Mech. Eng. 25 (2012) 1287–1297.
[6] P.M. Shi, X.J. Ding, D.Y. Han, Study on multi-frequency weak signal detection method based on stochastic resonance tuning by multi-scale noise, Measurement 47 (2014) 540–546.
[7] G.Y. Li, J.M. Li, S.B. Wang, X.F. Chen, Quantitative evaluation on the performance and feature enhancement of stochastic resonance for bearing fault diagnosis, Mech. Syst. Signal Process. 81 (2016) 108–125.
[8] R. Benzi, G. Parisi, A. Suter, A. Vulpiani, Stochastic resonance in climatic change, Tellus 34 (1982) 10–16.
[9] Y.G. Lei, D. Han, J. Lin, Z.J. He, Planetary gearbox fault diagnosis using an adaptive stochastic resonance method, Mech. Syst. Signal Process. 38 (2013) 113–124.
[10] J. Wang, Q.B. He, F.R. Kong, An improved multiscale noise tuning of stochastic resonance for identifying multiple transient faults in rolling element bearings, J. Sound Vib. 333 (2014) 7401–7421.
[11] Y. Qin, T. Tao, Y. He, B.P. Tang, Adaptive bistable stochastic resonance and its application in mechanical fault feature extraction, J. Sound Vib. 333 (2014) 7386–7400.
[12] X.H. Chen, G. Cheng, X.L. Shan, X. Hu, Q. Guo, H.G. Liu, Research of weak fault feature information extraction of planetary gear based on ensemble empirical mode decomposition and adaptive stochastic resonance, Measurement 73 (2015) 55–67.
[13] B.B. Hu, B. Li, A new multiscale noise tuning stochastic resonance for enhanced fault diagnosis in wind turbine drivetrains, Meas. Sci. Technol. 27 (2016). (025017_1-_14).
[14] Z.H. Lai, Y.G. Leng, Weak-signal detection based on the stochastic resonance of bistable Duffing oscillator and its application in incipient fault diagnosis, Mech. Syst. Signal Process. 81 (2016) 60–74.
[15] F.F. Seelig, Mono- or bistable behavior in a weakly or strongly open chemical reaction system, J. Theor. Biol. 32 (1971) 93–106.
[16] M. Evstigneev, P. Reimann, V. Pankov, R.H. Prince, Stochastic resonance in monostable overdamped systems, Europhys. Lett. 65 (2004) 7–12.
[17] S.B. Jiao, C. Ren, P.H. Li, Q. Zhang, G. Xie, Stochastic resonance in an overdamped monostable system with multiplicative and additive α stable noise, Acta Phys. Sin. 63 (2014). (070501_1-9).
[18] C.W. Duan, Y.F. Zhang, The response of a linear monostable system and its application in parameters estimation for PSK signals, Phys. Lett. A 380 (2016) 1358–1362.
[19] F. Guo, Stochastic resonance in a bias monostable system with frequency mixing force and multiplicative and additive noise, Phys. A 388 (2009) 2315–2320.
[20] N.V. Agudov, A.V. Krichigin, D. Valenti, B. Spagnolo, Stochastic resonance in a trapping overdamped monostable system, Phys. Rev. E 81 (2010). (051123_1-6).
[21] S.L. Lu, Q.B. He, H.B. Zhang, F.R. Kong, Enhanced rotating machine fault diagnosis based on time-delayed feedback stochastic resonance, J. Vib. Acoust. 137 (2015). (051008_1-12).
[22] N. Sawalhi, R.B. Randall, H. Endo, The enhancement of fault detection and diagnosis in rolling element bearings using minimum entropy deconvolution combined with spectral kurtosis, Mech. Syst. Signal Process. 21 (2007) 2616–2633.
[23] T. Barszcz, N. Sawalhi, Fault detection enhancement in rolling bearing using the minimum entropy deconvolution, Arch. Acoust. 37 (2012) 131–141.
[24] T.D. Frank, Delay Fokker-Planck equations, perturbation theory, and data analysis for nonlinear stochastic system with time delays, Phys. Rev. E 71 (2005). (031106_1-14).
[25] T.D. Fran, Delay Fokker-Planck equations, Novikov's theorem, and Boltzmann distributions as small delay approximations, Phys. Rev. E 72 (2005). (011112_1-8).
[26] S. Guillouzic, I. L'Heureux, A. Longtin, Small delay approximation of stochastic delay differential equations, Phys. Rev. E 59 (1999) 3970–3982.
[27] G. Hu, Stochastic Force And Nonlinear System, Shanghai Science and Technology Education Publishing House, Shanghai, 1994.
[28] R.A. Wiggins, Minimum entropy deconvolution, Geoexploration 16 (1978) 21–35.
[29] H. Endo, R.B. Randall, Enhancement of autoregressive model based gear tooth fault detection technique by the use of minimum entropy deconvolution filter, Mech. Syst. Signal Process. 21 (2007) 906–919.
[30] G.L. McDonald, Q. Zhao, M.J. Zuo, Maximum correlated kurtosis deconvolution and application on gear tooth chip fault detection, Mech. Syst. Signal Process. 33 (2012) 237–255.